Physica C: Superconductivity and its applications 571 (2020) 1353586

Contents lists available at ScienceDirect

Physica C: Superconductivity and its applications

journal homepage: www.elsevier.com/locate/physc

Investigation of the transport, magnetic and flux pinning properties of the noncentrosymmetric superconductor $TaRh_2B_2$ under hydrostatic pressure

S. Arumugam[a,*], N. Subbulakshmi[a], K. Manikandan[a], M. Kannan[a], D.A. Mayoh[b], M.R. Lees[b], G. Balakrishnan[b]

[a] Centre for High Pressure Research, School of Physics, Bharathidasan University, Tiruchirappalli 620024, Tamil Nadu, India
[b] Physics Department, University of Warwick, Coventry CV4 7AL, United Kingdom

ARTICLE INFO

Keywords:
Critical current density
Flux pinning
Non–centrosymmetric superconductors
Pressure effect

ABSTRACT

The bulk superconducting properties of polycrystalline $TaRh_2B_2$ under pressure are investigated with transport resistivity [$\rho(T)$], and dc magnetization [$M(T)$ and $M(H)$] measurements up to ~3 GPa, and 1 GPa respectively. The application of hydrostatic pressure leads to a decrease in T_c for both magnetic [dT_c/dP is −0.4 K/GPa ($0 \le P \le 1$ GPa)] and transport [(dT_c/dP) is −0.02 K/GPa ($0 \le P \le 1$ GPa) and −0.06 K/GPa ($1 \le P \le 2.5$ GPa)] measurements. At 2.5 GPa the upper critical field, $\mu_0 H_{c2}(0)$, and the irreversible field, $\mu_0 H_{irr}(0)$, are found to be (11.8 ± 0.2) T and (6.5 ± 0.1) T respectively. The critical current density, J_c (at $\mu_0 H = 0$ T), decreases from 6.5×10^5 A/cm^2 (0 GPa) to 2.5×10^5 A/cm^2 (0.9 GPa) at 4.3 K. The flux pinning and $J_c(H)$ in $TaRh_2B_2$ are significantly affected by the application of external pressure. It is seen that surface and volume flux pinning coexist both at ambient pressure and at high pressure. We infer that the pinning energy and superconducting properties are suppressed by external pressure.

1. Introduction

The family of unconventional superconductors has grown considerably over the last few decades and now includes the cuprates [1,2], heavy-fermions [3,4], iron pnictides [5–7], topological superconductors [8,9], and the noncentrosymmetric (NCS) superconductors [10–14]. Although noncentrosymmetric superconductors have been known for some time [15], the discovery of the heavy fermion superconductivity in $CePt_3Si$ [3] reignited interest in the role that the structure of a material plays in determining its superconducting properties. The absence of a center of inversion symmetry in a NCS superconductor produces an asymmetric electrical field gradient, which can split the previously two-fold degenerate spin electronic bands [10]. As a result, in NCS superconductors it is possible that a combination of even and odd parity Cooper pair states replaces the conventional spin-singlet or spin-triplet pairing [10]. A large number of NCS superconductors have now been investigated with many showing anomalous superconducting behavior [16].

Pressure (P) is an effective tool with which to alter both the electronic and crystal structure of a material. Pressure has been shown to have a significant impact on unconventional superconducting materials including in the cuprates [2], pnictides [7], 2D layer superconductors [17,18], BiS_2-based superconductor [19,20] and topological superconductors [9,21]. Studies under pressure have helped to build an understanding of the nature of the superconducting state in these different groups of materials. Pressure has also played a vital role in the study of noncentrosymmetric superconductors. Negative pressure coefficients, dT_c/dP, have been observed in La_7Ir_3 (−0.15 K/GPa) [13], $BaPtSi_3$ (−0.06 K/GPa) [22], and BiPd (−0.62 K/GPa) [23] suggesting s-wave singlet superconductivity. Positive pressure coefficients have been reported in $LaNiC_2$ (+0.25 K/GPa) [24] and Mo_3Al_2C (+0.28 K/GPa) [25]. The superconducting gap in $LaNiC_2$ has been reported to be a two gap ($s + +s$)-wave [26]. The nature of the superconducting gap in Mo_3Al_2C remains unclear. Specific heat measurements indicate the possibility of an unconventional anisotropic gap, [27] while muon spin rotation measurements on Mo_3Al_2C indicate an isotropic nodeless superconducting gap structure [28]. The positive pressure coefficients in $LaNiC_2$ and Mo_3Al_2C may be indicative of the exotic superconducting gap structures in these materials. The superconductivity ($T_c = 0.75$ K) and antiferromagnetic (AFM) order ($T_N = 2.2$ K) in $CePt_3Si$ are both suppressed by external pressure [29]. However, while T_N becomes zero at ~0.6 GPa, the superconducting phase is shown to exist up to 1.5 GPa. In $CeRhSi_3$, the superconducting state coexists with the AFM state at pressures of more than 1.2 GPa [4]. A superconducting state is induced

* **Corresponding author.**
E-mail address: sarumugam1963@yahoo.com (S. Arumugam).

https://doi.org/10.1016/j.physc.2019.1353586
Received 9 August 2019; Received in revised form 4 December 2019; Accepted 6 December 2019
Available online 06 December 2019
0921-4534/

by external pressure ($P > 2.63$ GPa) in ferromagnetic UIr [30]. Pressure induced superconductivity has also been observed at 1.8 GPa in $CeIrSi_3$ as the antiferromagnetic order is suppressed [31] and in $CeCoGe_3$ at 0.7 K and 5.5 GPa [32] and in $CeIrGe_3$ at 1.5 K at 20 GPa [33]. $TaRh_2B_2$ is one member of a new family of noncentrosymmetric superconductors with a chiral structure [11,12,14]. Here we report on the transport and magnetic properties under hydrostatic pressure of a polycrystalline sample of $TaRh_2B_2$. The pressure dependence of the superconducting transition temperature, upper and lower critical fields, irreversibility field, and the critical current density are all analyzed in order to gain a better understanding of the nature of the superconductivity in this new material.

2. Experimental details

Polycrystalline samples of $TaRh_2B_2$ were synthesized using the solid-state reaction method as described elsewhere [11,12]. These polycrystalline samples have previously been characterized by ac susceptibility, dc magnetization and resistivity and heat capacity measurements at various magnetic fields and temperatures at ambient pressure [12]. In this study the temperature dependent dc resistivity [$\rho(T)$], and magnetization, [$M(T)$ and $M(H)$], were measured at various pressures using a Quantum Design Physical Property Measurement System (PPMS). The electrical resistivity measurements were carried out using a piston type pressure cell at pressures of up to ~3 GPa with the pressure transmitting medium Daphne #7474. The pressure calibration was performed using the fixed pressure points of Bi. The dc magnetization measurements up to ~1 GPa were made using a hybrid clamp-type miniature pressure cell with the pressure transmitting medium mixture of fluorinert FC#70 and FC#77(1:1). Here the applied pressure in the cell was determined from the change of T_c in pure Sn. Several studies have shown that the pressure transmitting medium used produces a hydrostatic pressure up to about 3 GPa [17,19,34].

3. Results and discussions

Fig. 1(a) presents the temperature dependent electrical resistivity, $\rho(T)$, in the temperature range 5.5–6.5 K under various hydrostatic pressures, P, from 0 to 2.5 GPa. The observation of a sharp superconducting transition temperature, T_c, and zero resistivity at every pressure is indicative of the hydrostatic nature of pressure in this sequence of measurements. The $T_c \sim 6$ K along with very low residual resistivity ratio (RRR) $\rho^{300\ K}/\rho^{10\ K} \sim 1$ at ambient pressure are in good agreement with previous measurements [11,12]. The normal state resistivity at room temperature, ρ^{RT}, and the temperature of the onset of the superconducting transition, $\rho^{Tc(onset)}$, are both sensitive to the application of external pressure. ρ^{RT} and $\rho^{Tc(onset)}$ decrease at rates of 0.097 mΩ-cm/GPa and 0.007 mΩ-cm/GPa, respectively, up to 2.5 GPa. The superconducting transition temperature also decreases with pressure. The superconducting onset transition temperature, T_c^{onset}, is found from the intersection of two straight lines, one drawn on the resistivity curve above the transition, and the other at the steepest section of the transition to the superconducting state. The superconducting midpoint transition temperature, T_c^{mid}, is found from the peak positions of the $d\rho(T)/dT$ versus T curves and T_c^{zero} is determined from the zero resistivity. The results show that T_c decreases monotonically with the application of pressure as shown in Fig. 1(c). The almost parallel shift in the resistivity curves in the vicinity of superconducting transition mean T_c^{onset}, T_c^{mid} and T_c^{zero} all decrease monotonically with the application of external pressure. The pressure dependence of T_c^{mid} is $dT_c/dP = -0.02$ K/GPa for $0 \le P \le 1$ GPa and -0.06 K/GPa for $1 \le P \le 2.5$ GPa. The negative pressure coefficient of T_c indicates that there is a phonon-mediated BCS-like pairing mechanism for $TaRh_2B_2$. Similar rates of change in T_c have been observed in other noncentrosymmetric superconductors such as $BaPtSi_3$ (-0.06 K/GPa) [22], while slightly higher values are found in other NCS materials, for example, La_7Ir_3 (-0.15 K/GPa) [13] and BiPd (-0.62 K/GPa) [23].

The temperature dependence of the dc magnetization, $M(T)$, was measured in an applied field of 1 mT in zero-field cooled (ZFC) and field-cooled cooling (FCC) modes at various hydrostatic pressures up to ~1 GPa (see Fig. 1(b)). With decreasing temperature, both the FCC and ZFC magnetization curves deviate from the normal-state behavior due to the onset of diamagnetism, signaling the occurrence of superconductivity. Below T_c the magnetization drops sharply. The splitting of the ZFC and FCC data is typical for a type-II superconductor. Bulk superconductivity is observed at 6.02 and 5.62 K at ambient pressure and 0.9 GPa respectively and the $T_c(P)$ values listed in Table 2, giving a rate of change of T_c with P of -0.44 K/GPa ($0 \le P \le 0.9$ GPa). The $\rho(T)$ curves for $TaRh_2B_2$ in different magnetic fields, H, under various fixed pressures are shown in Figs. 1(c–e). T_c in each $\rho(T)$ curve is found from the peak in the $d\rho/dT$. With increasing H, the transition width, $\Delta T_c = T_c^{onset} - T_c^{zero}$, in the resistivity data becomes broader and the onset of superconductivity progressively shifts to low temperatures. $M(T)$ measurements for $TaRh_2B_2$ made in different magnetic fields at 0, 0.6 and 0.9 GPa are shown in Fig. 2(a–c). Figs. 2(d–f) present the field dependent isothermal magnetization versus field curves at 0, 0.6, and 0.9 GPa. The signal (Meissner fraction) decreases with increasing magnetic field and external pressure. The superconducting transition under pressure is sharper than that observed for some other superconducting materials [17,18,35,36]. The width of the superconducting hysteresis loop at each temperature decreases with the application of pressure and there is a diamagnetic background that increases with pressure. These data indicate that the pinning strength in this polycrystalline sample of $TaRh_2B_2$ decreases as the pressure is increased.

The data presented above can be combined to produce the H-T and H-P phase diagrams for the superconducting state of $TaRh_2B_2$ shown in Figs. 3(a–d). The temperature dependence of the upper critical field, $H_{c2}(T)$, at several pressures is shown in Fig. 3(a), where the T_c at each field is calculated from the peak position in the $d\rho(T)/dT$ curves. The orbital upper critical field, $H_{c2}^{orb}(0)$, can be determined from the Werthamer-Helfand-Hohenberg (WHH) model [37], $H_{c2}^{orb}(0) = -0.693 T_c [dH_{c2}/dT]_{T=T_c}$ for the dirty limit. The $H_{c2}^{orb}(0)$ decreases from 12.9 T at 0 GPa to 9.2 T under a pressure of 2.5 GPa (see Table 1). In the conventional Ginzburg-Landau theory, the upper critical field, $H_{c2}(0)$, can be estimated using $H_{c2}(0) = H_{c2}(0)((1-t^2)/(1+t^2))$, where $t = T/T_c$. Fits using this expression are shown in Fig. 3(a). The $\mu_0 H_{c2}(0)$ values range from 15.2 T at ambient pressure to 11.8 T at 2.5 GPa. The Pauli-Clogston limiting field, $H_p(0) = 1.84 T_c$ [38]. As T_c decreases with pressure, the value of $H_p(0)$ also decreases, as shown in Table 1. We can use the Maki parameter, $\alpha = \sqrt{2} H_{c2}^{orb}(0)/H_p(0)$ [39], the ratio of the orbital and Pauli limiting fields, as a gauge of the relative importance of Pauli spin paramagnetic and orbital pair breaking effects. In a conventional superconductor, a value of $\alpha > 1$ may be taken to indicate that Pauli paramagnetic pair breaking effects are considerable. In $TaRh_2B_2$, however, while $\alpha > 1$ for all pressures, we find that $H_p(0) < H_{c2}^{orb}(0) < H_{c2}(0)$ and similar effects observed $CeIrSi_3$ superconductor under P [31]. Therefore, we must also consider the effects of strong spin-orbit scattering. For a fixed value of α, any increase in the spin-orbit scattering parameter, λ_{SO}, increases $H_{c2}(0)$. Furthermore, $TaRh_2B_2$ is suggested to be a multi band superconductor [12]. In this scenario, inter and intra band scattering effects also need to be considered. A complete explanation of the temperature dependence of H_{c2} will require studies on single crystal samples. $H_{irr}(T)$ curves under pressure for $TaRh_2B_2$ were determined from resistivity data. The $H_{irr} - T$ data points were taken to be the fields and temperatures at which the sample first exhibited zero resistivity. $H_{irr}(T)$ is well fit using the empirical relationship $H_{irr}(T) = H_{irr}(0)(1 - t^2)^{1.5}$, where $t = T/T_c$, as shown in Fig. 3(b). The estimated value for $\mu_0 H_{irr}(0)$ decreases from 7.84 T to 6.5 T at 2.5 GPa. This is an indication that $H_{irr}(0)$ is predominantly determined by the strength of the flux pinning that also appears to decrease with pressure. In order to determine the lower

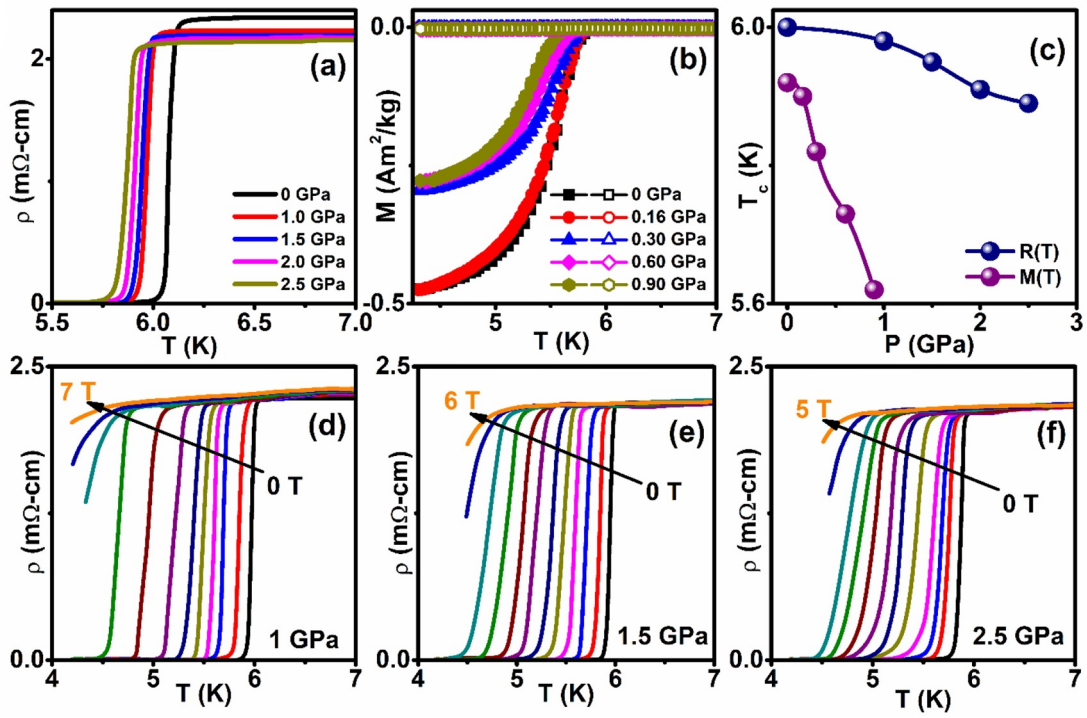

Fig. 1. (a) Temperature dependence of the electrical resistivity for $TaRh_2B_2$ under various hydrostatic pressures up to 2.5 GPa. **(b)** Temperature dependence of the zero-field cooled (ZFC) and field-cooled cooling (FCC) magnetization in an applied field of 1 mT for $TaRh_2B_2$ under hydrostatic pressures of up to ~ 1 GPa. **(c)** Pressure dependence of the superconducting critical temperature, T_c. **(d)-(f)** Temperature dependence of electrical resistivity for $TaRh_2B_2$ in different magnetic fields and hydrostatic pressures.

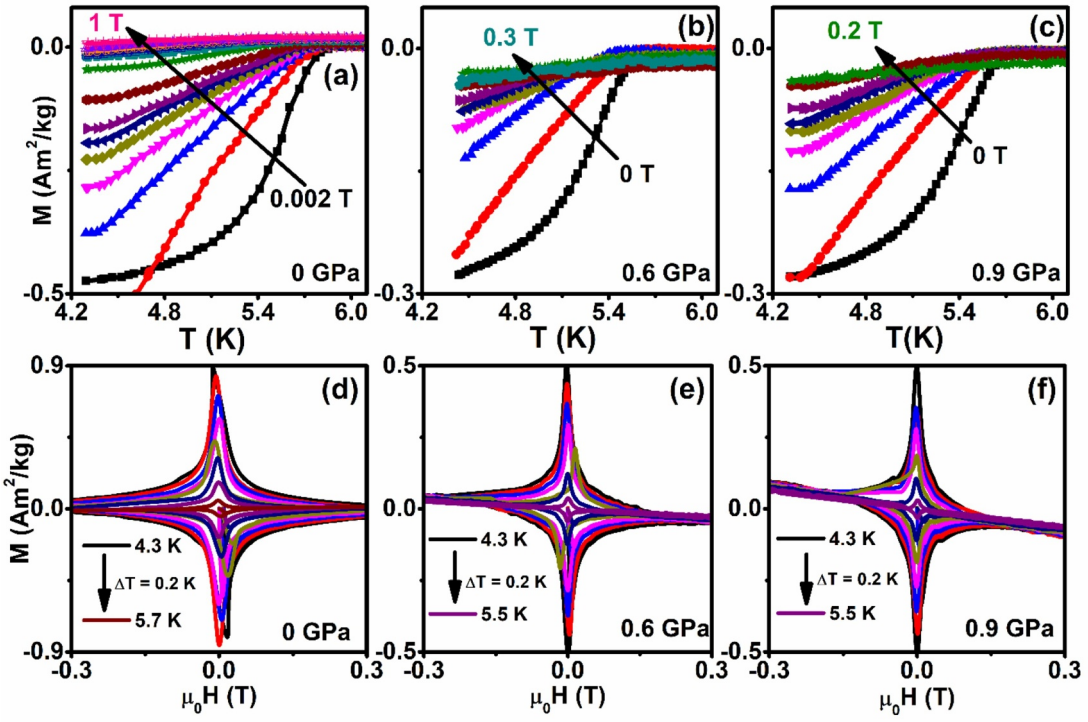

Fig. 2. (a)-(c) Temperature dependence of the dc magnetization of $TaRh_2B_2$ measured in various magnetic fields at 0, 0.6, and 0.9 GPa (d)-(e) Field dependent $M(H)$ loops for $TaRh_2B_2$ measured at different temperatures under pressures of 0, 0.6, and 0.9 GPa.

critical field, H_{c1}, from $M(H)$ measurements, the applied fields need to be corrected for demagnetization effects. H_{c1} can then be deduced from the first penetration field H^*_{c1}, assuming that the magnetization $M = -H_{c1}$ when the first vortex enters the sample. According to Brandt's formulation, $H_{c1}(T) = H^*_{c1}(T)/\tanh\sqrt{(0.36b/l)}$ for a slab geometry, where b and l are the width and length of the samples respectively [40]. Using this criterion, a set of $H_{c1}(T)$ values was estimated and fit with a parabolic GL temperature dependence, $H_{c1}(T) = H_{c1}(0)$

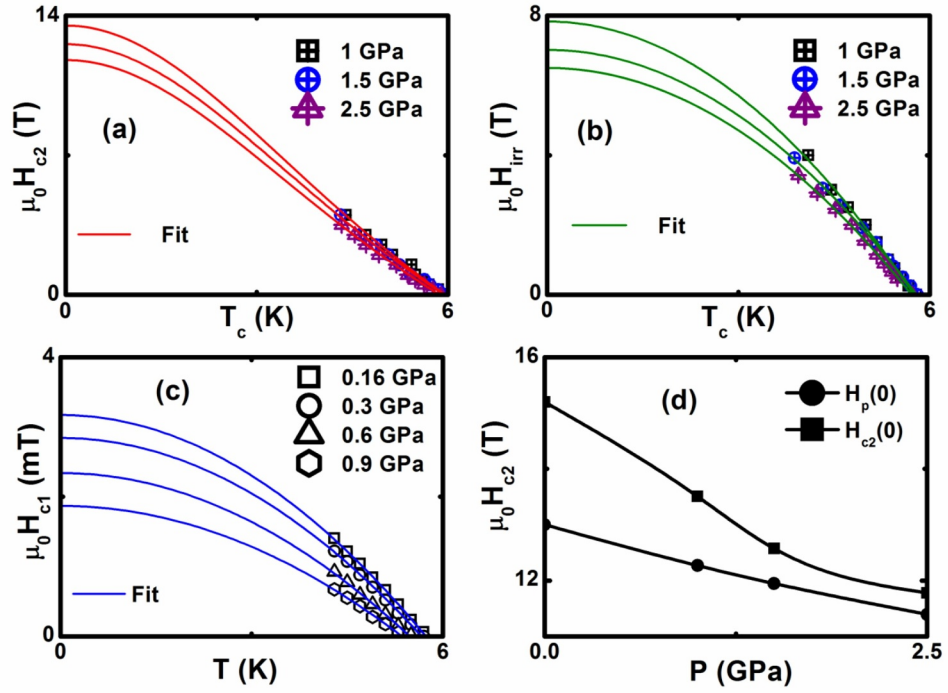

Fig. 3. (a) Temperature dependence of the upper critical field, $H_{c2}(T)$ for a polycrystalline sample of $TaRh_2B_2$. The solid lines are fits made using the Ginzburg–Landau equation $H_{c2}(T) = H_{c2}(0)[(1-t^2)/((1+t^2)]$. **(b)** Irreversibility field (H_{irr}) as a function of temperature for $TaRh_2B_2$. The solid lines are fits with the empirical relationship $H_{irr}(T) = H_{irr}(0)(1-t^2)^{1.5}$. H_{c2} and H_{irr} were determined from $\rho(T)$ measurements under pressure. **(c)** Temperature dependence of the lower critical field, H_{c1}, calculated from $M(H)$ measurements at various pressures. Solid lines are fits with a parabolic function. **(d)** Pressure dependence of the upper critical field and the Pauli limiting field at absolute zero for $TaRh_2B_2$. $H_{c2}(0)$ was determined from the fits to $H_{c2}(T)$ shown in Fig. 3(a).

$[1-t^2]$ as shown in the Fig. 3(c). The estimated lower critical field decreases from a value 4 mT at 0 GPa (in good agreement with the $H_{c1}(0)$ reported in [12]), to 1.87 mT at 0.9 GPa and the $H_{c1}(P)$ values are tabulated in Table 2.

The Ginzburg-Landau coherence length, $\xi_{GL}(0)$, can be estimated from the $H_{c2}(0)$ using the relation, $\xi_{GL}(0) = \sqrt{\Phi_0/2\pi H_{c2}(0)}$, where $\Phi_0 = 2.07 \times 10^{-15}$ Wb. The calculated values of $\xi_{GL}(0)$ at various pressures are given in Table 1. The value in zero field agrees with that reported in Ref. [12]. The coherence length of $TaRh_2B_2$ at 2.5 GPa is comparable with the NCS superconductor $CeIrSi_3$ (5.4 nm at 2.5 GPa) [31], where the application of pressure first suppresses AFM order, before eventually leading to superconductivity with a similar $H_c(0)$, albeit with a much lower T_c. The magnetic field dependence of the critical current density, J_c, for $TaRh_2B_2$ at 4.3 K under different pressures is shown in the Fig. 4(a). The J_c values are extracted from the magnetic hysteresis loops using the Bean model [41,42] with $J_c(H) = 20\Delta M/\{l(1-(l/3b))\}$ where ΔM is the width of the superconducting hysteresis loop. J_c decreases under pressure and the value of $J_c(0)$ at ambient pressure is reduced by a factor of ~3 at 0.9 GPa and the $J_c(P)$ shows in Table 2. J_c drops quickly at higher magnetic fields at ambient and high pressure. Fig. 4(b) shows the pressure dependence of J_c at 4.3 K in various magnetic fields. The solid lines are linear fits to the experimental data, which give negative slopes with $|d(\ln J_c)/dP|$ of 1, 1.5, 2.12 and 3.33 GPa^{-1} at magnetic fields of 0, 0.05, 0.1, and 0.2 T respectively, indicating that the effects of pressure in decreasing J_c are more substantial at higher magnetic fields. Fig. 4(c) shows J_c as a function of magnetic field at 4.3 K under hydrostatic pressures from 0 to 0.9 GPa on a log-log scale. J_c decreases exponentially as a function of magnetic field and the expression, $J_c(H) = J_c(H=0)\exp(-H/H_0)^{3/2}$ produces excellent fits to the data, as shown in Fig. 4(c). As can be seen from the plateau region at lower magnetic field, initially J_c shows a weak dependence with applied field. As the field is increased beyond a crossover field, J_c decreases more quickly. J_c drops even more rapidly in the field regime close to the irreversibility field. The crossover field decreases with increasing temperature as seen from the isothermal magnetic hysteresis loops. The magnetic field dependence of the pinning force (F_p) assessed using the relation $F_p(H) = J_c(H) \times H$ at 4.3 K and the normalized pinning force ($f_p = F_p/F_p^{max}$) as a function of reduced magnetic field ($h = H/H_{irr}^K$) under various hydrostatic pressures are shown in Fig. 4(d) [43]. The results suggest that an external pressure decreases the number of point pinning centres, and diminishes the total pinning force. Fitting the data using the Dew-Hughes model [43], $f_p \propto h^m(1-h)^n$, where m and n are fitting parameters, provides an indication of the nature of flux pinning mechanism. From this model, $n \approx 0.5$ and $m \approx 2$ indicates surface pinning while $n \approx 0.5$ and $m \approx 1$ describes volume pinning, as predicted by Kramer [44]. The irreversibility fields, H_{irr}^K, were determined from linear interpolations of

Table 2
Lower critical field and the critical current density in zero field obtained from width of the hysteresis loops at 4.3 K as a function of pressure for $TaRh_2B_2$.

Pressure [GPa]	T_c^{on} [K]	$\mu_0 H_{c1}(0)$ [mT]	$J_c(0)$ at 4.3 K 10^5 A/cm^2
0	6.02	4.0 ± 0 .05	6.5
0.16	5.90	3.17 ± 0.03	5.3
0.3	5.82	2.84 ± 0.02	4.3
0.6	5.73	2.34 ± 0.03	3.3
0.9	5.62	1.87 ± 0.01	2.5

Table 1
Superconducting parameters for $TaRh_2B_2$ obtained from the resistivity and magnetization measurements made under pressure.

Pressure [GPa]	T_c^{zero} [K]	$H_{c2}^{orb}(0)$ [T]	$\mu_0 H_{c2}(0)$ [T]	$\mu_0 H_p(0)$ [T]	α	$\mu_0 H_{irr}(0)$ [T]	$\xi_{GL}(0)$ [nm]
0	6.02	12.9	15.2 ± 0.1	13	1.65	–	4.67
1	5.98	10.5	13.5 ± 0.1	12.3	1.56	7.84 ± 0.2	4.9
1.5	5.95	9.8	12.6 ± 0.1	11.9	1.49	7 ± 0.1	5.1
2.5	5.5	9.2	11.8 ± 0.2	11.4	1.46	6.5 ± 0.1	5.3

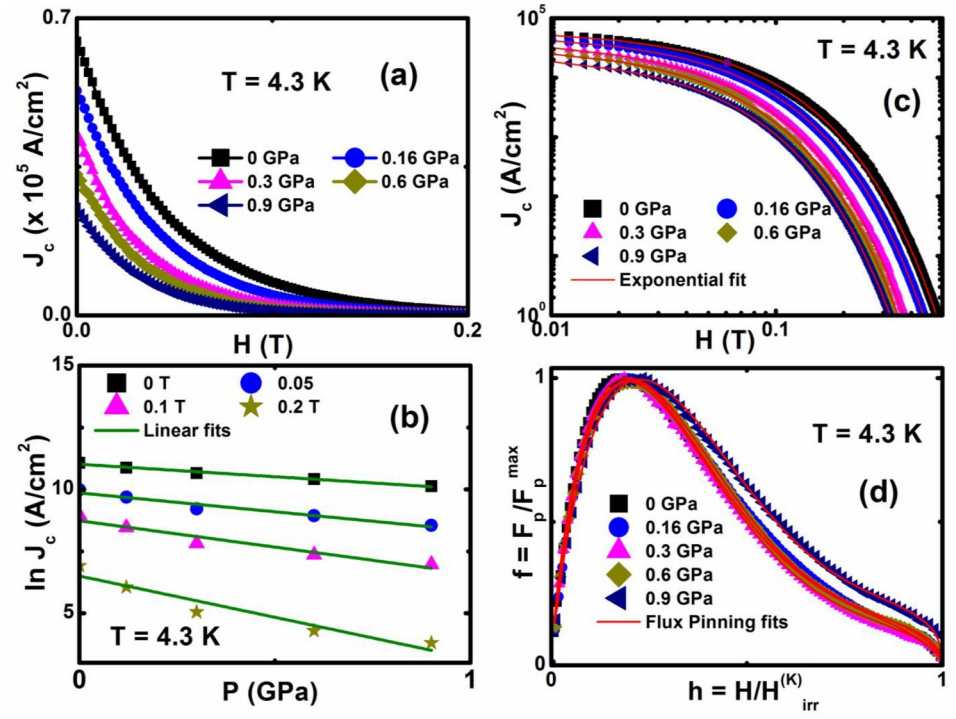

Fig. 4. (a) Magnetic field dependence of the critical current density, J_c, for $TaRh_2B_2$ under various pressures measured at 4.3 K. **(b)** Pressure dependence of the logarithm of the critical current density (T = 4.3 K) at various magnetic fields. The solid lines are linear fits to the data. **(c)** Field dependence of the critical current density at 4.3 K under various pressures on a log-log scale. The fits (solid lines) show that the critical current density decays exponentially. **(d)** Normalized vortex pinning force versus reduced magnetic field in $TaRh_2B_2$ under various pressures at 4.3 K. The solid lines are fits made using the Dew–Hughes model.

$J_c^{0.5}H^{0.25}$ versus H curves (Kramer plots). We found this theoretical formalism is in good agreement with the experimental data at 4.3 K and that surface and volume pinning coexist at ambient and high pressures. The best fits are obtained with normalized $f_p(h)$ given by, $Ah^{0.74}(1 - h)^{4.1} + Bh^{0.6}(1 - h)^{0.87}$ at ambient pressure and $Ah^{0.69}(1 - h)^{3.3} + Bh^{0.4}(1 - h)^{0.7}$ at a pressure of 0.9 GPa. Fitting parameters that lie in the range $0.69 \leq m \leq 0.74$, $3.3 \leq n \leq 4.1$ indicate surface pinning while for volume pinning $0.4 \leq m \leq 0.6$ and $0.7 \leq n \leq 0.87$. When the applied field is perpendicular to the surface, these grain boundaries are the main pinning centers and provide surface pinning. Both the surface and volume pinning decrease as a result of the application of external pressure.

4. Summary

In summary, we have systematically examined the effects of external hydrostatic pressure on the transport and magnetic properties of polycrystalline samples of the noncentrosymmetric superconductor $TaRh_2B_2$. We find that the superconducting parameters T_c, H_{c2}, H_{irr}, H_{c1}, J_c and F_p all decrease with the application of pressure. The superconducting transition temperature determined from the $\rho(T)$ measurements decreases with a pressure coefficient, dT_c/dP, of -0.02 K/GPa ($0 \leq P \leq 1$ GPa) and -0.06 K/GPa ($1 \leq P \leq 2.5$ GPa). The flux pinning force shows that surface and volume pinning coexist under ambient and high pressure. Both types of pinning decrease due to the reduction in the pinning centers by external pressure in $TaRh_2B_2$. These results indicate that $TaRh_2B_2$ is a phonon-mediated BCS-like superconductor. Examining the data presented here and in Refs. [11,12] there is no clear evidence for mixed-parity superconductivity in $TaRh_2B_2$. The superconducting gap appears to be dominated by an s-wave component making it difficult to identify any parity mixing. High quality single crystals of $TaRh_2B_2$ are required to look for stronger evidence of anisotropies in the superconducting gap.

Author statement

We thank the reviewers for their valuable suggestions for improving the overall quality of the manuscript. We have replied to the reviewers' comments, made modifications to the manuscript and have provided a revised manuscript. We hope that you will now consider our revised manuscript for publication in your journal.

Declaration of Competing Interest

There is no conflict on interest in this manuscript.

Acknowledgements

The author K.M. thanks to University Grant Commission, New Delhi, India (UGC-RGNF) for his research fellowship. S.A. acknowledges the DST (FIST, PURSE), SERB, New Delhi and UGC-DAE-CSR, Indore. M.K. wishes to thank CSIR for the award of research fellowship. The work at the University of Warwick was supported by EPSRC, UK, through Grant EP/M028771/1.

Supplementary materials

Supplementary material associated with this article can be found, in the online version, at doi:10.1016/j.physc.2019.1353586.

References

[1] M. Le Tacon, A. Bosak, S.M. Souliou, G. Dellea, T. Loew, R. Heid, K.-.P. Bohnen, G. Ghiringhelli, M. Krisch, B. Keimer, Inelastic X-ray scattering in $YBa_2Cu_3O_{6.6}$ reveals giant phonon anomalies and elastic central peak due to charge-density-wave formation, Nat. Phys. 10 (2013) 52–58 https://doi.org/10.1038/nphys2805.

[2] A. Yamamoto, N. Takeshita, C. Terakura, Y. Tokura, High pressure effects revisited for the cuprate superconductor family with highest critical temperature, Nat. Commun. 6 (2015) 89990 https://doi.org/10.1038/ncomms9990.

[3] E. Bauer, G. Hilscher, H. Michor, C. Paul, E.W. Scheidt, A. Gribanov, Y. Seropegin, H. Noël, M. Sigrist, P. Rogl, Heavy fermion superconductivity and magnetic order in noncentrosymmetric $CePt_3Si$, Phys. Rev. Lett. 92 (2004) 027003https://doi.org/10.1103/PhysRevLett.92.027003.

[4] N. Kimura, K. Ito, K. Saitoh, Y. Umeda, H. Aoki, T. Terashima, Pressure-induced superconductivity in noncentrosymmetric Heavy–Fermion $CePt_3Si$, Phys. Rev. Lett. 95 (2005) 247004https://doi.org/10.1103/PhysRevLett.95.247004.

[5] F. Hunte, J. Jaroszynski, A. Gurevich, D.C. Larbalestier, R. Jin, A.S. Sefat, M.A. McGuire, B.C. Sales, D.K. Christen, D. Mandrus, Two-band superconductivity in $LaFeAsO_{0.89}F_{0.11}$ at very high magnetic fields, Nature 453 (2008) 903–905 https://doi.org/10.1038/nature07058.

[6] S. Khim, J.W. Kim, E.S. Choi, Y. Bang, M. Nohara, H. Takagi, K.H. Kim, Evidence for dominant Pauli paramagnetic effect in the upper critical field of single-crystalline $FeTe_{0.6}Se_{0.4}$, Phys. Rev. B. 81 (2010) 184511https://doi.org/10.1103/PhysRevB.81.184511.

[7] S. Arumugam, C. Ganguli, R. Thiyagarajan, D. Bhoi, G.K. Selvan, K. Manikandan, A. Pariari, P. Mandal, Y. Uwatoko, Effect of pressure on normal and superconducting state properties of iron based superconductor $PrFeAsO_{0.6}F_y$ (y = 0.12, 0.14), Sci. Rep. 7 (2017) 11731 https://doi.org/10.1038/s41598-017-11927-1.

[8] T.V. Bay, T. Naka, Y.K. Huang, H. Luigjes, M.S. Golden, A. de Visser, Superconductivity in the doped topological insulator $Cu_xBi_2Se_3$ under high pressure, Phys. Rev. Lett. 108 (2012) 057001https://doi.org/10.1103/PhysRevLett.108.057001.

[9] K. Manikandan, Shruti, P. Neha, G. Kalai Selvan, B. Wang, Y. Uwatoko, K. Ishigaki, R. Jha, V.P.S. Awana, S. Arumugam, S. Patnaik, Possibility for conventional superconductivity in $Sr_{0.1}Bi_2Se_3$ from high-pressure transport studies, Europhys. Lett. 118 (2017) 47008 https://doi.org/10.1209/0295-5075/118/47008.

[10] P. Frigeri, D.F. Agterberg, A. Koga, M. Sigrist, Superconductivty without inversion symmetry: MnSi versus $CePt_3Si$, Phys. Rev. Lett. 92 (2004) 097001https://doi.org/10.1103/PhysRevLett.92.097001.

[11] E.M. Carnicom, W. Xie, T. Klimczuk, J. Lin, K. Górnicka, Z. Sobczak, N.P. Ong, R.J. Cava, $TaRh_2B_2$ and $NbRh_2B_2$: superconductors with a chiral noncentrosymmetric crystal structure, Sci. Adv. 4 (2018) eaar7969 https://doi.org/10.1126/sciadv.aar7969.

[12] D.A. Mayoh, A.D. Hillier, K. Götze, D.M.K. Paul, G. Balakrishnan, M.R. Lees, Multigap superconductivity in chiral noncentrosymmetric $TaRh_2B_2$, Phys. Rev. B. 98 (2018) 014502https://doi.org/10.1103/PhysRevB.98.014502.

[13] B. Li, C.Q. Xu, W. Zhou, W.H. Jiao, R. Sankar, F.M. Zhang, H.H. Hou, X.F. Jiang, B. Qian, B. Chen, A.F. Bangura, X. Xu, Evidence of s -wave superconductivity in the noncentrosymmetric La_7Ir_3, Sci. Rep. 8 (2018) 651 https://doi.org/10.1038/s41598-017-19042-x.

[14] D.A. Mayoh, M.J. Pearce, K. Götze, A.D. Hillier, G. Balakrishnan, M.R. Lees, Superconductivity and the upper critical field in the chiral noncentrosymmetric superconductor $NbRh_2B_2$, J. Phys. Condens. Matter. 31 (2019) 465601https://doi.org/10.1088/1361-648X/ab348b.

[15] B. Matthias, V. Compton, E. Corenzwit, Some new superconducting compounds, J. Phys. Chem. Solids 19 (1961) 130–133.

[16] M. Smidman, M.B. Salamon, H.Q. Yuan, D.F. Agterberg, Superconductivity and spin-orbit coupling in non-centrosymmetric materials: a review, Reports Prog. Phys. 80 (2017), https://doi.org/10.1088/1361-6633/80/3/036501.

[17] S. Arumugam, K. Manikandan, K. Ishigaki, J. Gouchi, R. Pervin, G.K. Selvan, P.M. Shirage, Y. Uwatoko, Enhancement of superconducting properties and flux pinning mechanism on Cr0.0005NbSe2 single crystal under hydrostatic pressure, Sci. Rep. 9 (2019) 347 https://doi.org/10.1038/s41598-018-36672-x.

[18] K. Manikandan, R. Pervin, K.S. Ganesan, K. Murugesan, G. Lingannan, A.K. Verma, P.M. Shirage, A. Sonachalam, Pressure assisted enhancement in superconducting properties of Fe substituted NbSe2 single crystal, Sci. Rep. 8 (2018) 1251 https://doi.org/10.1038/s41598-018-19636-z.

[19] G. Kalai Selvan, G.S. Thakur, K. Manikandan, A. Banerjee, Z. Haque, L.C. Gupta, A.K. Ganguli, S. Arumugam, Superconductivity in $La_{1-x}Sm_xO_{0.5}F_{0.5}BiS_2$(x = 0.2, 0.8) under hydrostatic pressure, J. Phys. D. Appl. Phys. 49 (2016) 275002https://doi.org/10.1088/0022-3727/49/27/275002.

[20] N. Subbulakshmi, G. Kalai Selvan, K. Manikandan, M. Kannan, Z. Haque, L.C. Gupta, A.K. Ganguli, Effect of hydrostatic pressure on $Eu_{3-x}Sr_xBi_2S_{4-y}Se_yF_4$ (x = 1 and 2 and y = 1 . 5 and 2) superconductors, J. Supercond. Nov. Magn. 4 (2019).

[21] R. Sankar, G.N. Rao, I.P. Muthuselvam, T.R. Chang, H.T. Jeng, G.S. Murugan, W.L. Lee, F.C. Chou, Anisotropic superconducting property studies of single crystal $PbTaSe_2$, J. Phys. Condens. Matter. 29 (2017), https://doi.org/10.1088/1361-648X/aa4edb.

[22] E. Bauer, R.T. Khan, H. Michor, E. Royanian, W. Wolf, M. Marsman, $BaPtSi_3$: a noncentrosymmetric BCS-like superconductor, Phys. Rev. B. 80 (2009) 064504https://doi.org/10.1103/PhysRevB.80.064504.

[23] R. Jha, R. Goyal, P. Neha, V.K. Maurya, A.K. Srivastava, A. Gupta, S. Patnaik, V.P.S. Awana, Weak ferromagnetism in a noncentrosymmetric BiPd 4K superconductor, Supercond. Sci. Technol. 29 (2016) 025008https://doi.org/10.1088/0953-2048/29/2/025008.

[24] S. Katano, H. Nakagawa, K. Matsubayashi, Y. Uwatoko, H. Soeda, T. Tomita, H. Takahashi, Anomalous pressure dependence of the superconductivity in non-centrosymmetric $LaNiC_2$: evidence of strong electronic correlations, Phys. Rev. B. 90 (2014) 220508https://doi.org/10.1103/PhysRevB.90.220508.

[25] E. Bauer, G. Rogl, X.-Q. Chen, R.T. Khan, H. Michor, G. Hilscher, E. Royanian, K. Kumagai, D.Z. Li, Y.Y. Li, R. Podloucky, P. Rogl, Unconventional superconducting phase in the weakly correlated noncentrosymmetric Mo_2Al_2C compound, Phys. Rev. B. 82 (2010) 064511https://doi.org/10.1103/PhysRevB.82.064511.

[26] J. Chen, L. Jiao, J.L. Zhang, Y. Chen, L. Yang, M. Nicklas, F. Steglich, H.Q. Yuan, Evidence for two-gap superconductivity in the non-centrosymmetric compound $LaNiC_2$, New J. Phys. 15 (2013) 053005https://doi.org/10.1088/1367-2630/15/5/053005.

[27] A.B. Karki, Y.M. Xiong, I. Vekhter, D. Browne, P.W. Adams, D.P. Young, K.R. Thomas, J.Y. Chan, H. Kim, R. Prozorov, Structure and physical properties of the noncentrosymmetric superconductor Mo_3Al_2C, Phys. Rev. B. 82 (2010) 064512https://doi.org/10.1103/PhysRevB.82.064512.

[28] E. Bauer, C. Sekine, U. Sai, P. Rogl, P.K. Biswas, A. Amato, Absence of time-reversal symmetry breaking in the noncentrosymmetric superconductor Mo_3Al_2C, Phys. Rev. B. 90 (2014) 054522https://doi.org/10.1103/PhysRevB.90.054522.

[29] N. Tateiwa, Y. Haga, T.D. Matsuda, S. Ikeda, T. Yasuda, T. Tetsuya, R. Settai, Y. Onuki, Novel pressure phase diagram of heavy fermion superconductor $CePt_3Si$ investigated by ac calorimetry, J. Phys. Soc. Japan. 74 (2005) 1903–1906 https://doi.org/10.1143/JPSJ.74.1903.

[30] T.C. Kobayashi, S. Fukushima, H. Hidaka, H. Kotegawa, T. Akazawa, E. Yamamoto, Y. Haga, R. Settai, Y. Onuki, Pressure-induced superconductivity in ferromagnet UIr without inversion symmetry, Phys. B. 378–380 (2006) 355–358 https://doi.org/10.1016/j.physb.2006.01.126.

[31] I. Sugitani, Y.O. Kuda, H.S. Hishido, T.Y. Amada, Pressure-Induced heavy-fermion superconductivity in antiferromagnet $CeIrSi_3$ without inversion symmetry, J. Phys. Soc. Japan. 75 (2006) 043703https://doi.org/10.1143/JPSJ.75.043703.

[32] R. Settai, I. Sugitani, Y. Okuda, A. Thamizhavel, M. Nakashima, Y. Onuki, H. Harima, Pressure-induced superconductivity in $CeCoGe_3$ without inversion symmetry, J. Magn. Magn. Mater. 310 (2007) 844–846 https://doi.org/10.1016/j.jmmm.2006.10.717.

[33] F. Honda, I. Bonalde, K. Shimizu, S. Yoshiuchi, Y. Hirose, T. Nakamura, R. Settai, Y. Onuki, Pressure-induced superconductivity and large upper critical field in the noncentrosymmetric antiferromagnet $CeIrGe_3$, Phys. Rev. B. 81 (2010) 140507https://doi.org/10.1103/PhysRevB.81.140507.

[34] N. Mori, H. Takahashi, N. Takeshita, Low-temperature and high-pressure apparatus developed at ISSP, University of Tokyo, High Press. Res. 24 (2004) 225–232 https://doi.org/10.1080/08957950410001661909.

[35] T. Akazawa, H. Hidaka, H. Kotegawa, T.C. Kobayashi, T. Fujiwara, E. Yamamoto, Y. Haga, R. Settai, Y. Ōnuki, Pressure-induced superconductivity in UIr, J. Phys. Soc. Japan. 73 (2004) 3129–3134 https://doi.org/10.1143/JPSJ.73.3129.

[36] Y. Aoki, A. Sumiyama, G. Motoyama, A. Yamaguchi, Y. Oda, T. Yasuda, R. Settai, Y. Onuki, Origin of high-Tcinclusion in noncentrosymmetric superconductor $CePt_3Si$, J. Phys. Soc. Japan. 80 (2011) 065001https://doi.org/10.1143/JPSJ.80.065001.

[37] N.R. Werthamer, E. Helfand, P.C. Hohenberg, Temperature and purity dependence of the superconducting critical field, Hc2. III. electron spin and spin-orbit effects, Phys. Rev. 147 (1966) 295–302 https://doi.org/10.1103/PhysRev.147.295.

[38] A.M. Clogston, Upper limit for the critical field in hard superconductors, Phys. Rev. Lett. 9 (1962) 266–267 https://doi.org/10.1103/PhysRevLett.9.266.

[39] K. Maki, Effect of pauli paramagnetism on magnetic properties of high-field superconductors, Phys. Rev. 148 (1966) 362–369 https://doi.org/10.1103/PhysRev.148.362.

[40] E.H. Brandt, Irreversible magnetization of pin-free type-II superconductors, Phys. Rev. B. 60 (1999) 11939–11942 https://doi.org/10.1103/PhysRevB.60.11939.

[41] C.P. Bean, Magnetization of hard superconductors, Phys. Rev. Lett. 8 (1962) 250–253 https://doi.org/10.1103/PhysRevLett.8.250.

[42] C.P. Bean, Magnetization of high-field superconductors, Rev. Mod. Phys. 36 (1964) 31–39 https://doi.org/10.1103/RevModPhys.36.31.

[43] D. Dewhughe, Flux pinning mechanisms in type-II superconductors, Philos. Mag. 30 (1974) 293–305.

[44] E.J. Kramer, Scaling laws for flux pinning in hard superconductors, J. Appl. Phys. 44 (1973) 1360–1370 https://doi.org/10.1063/1.1662353.